Accepted Manuscript

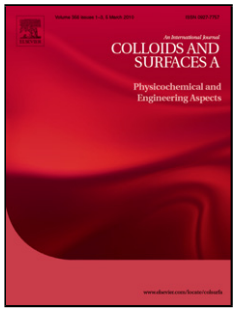

Title: *Click*–based thiol-ene photografting of COOH groups to SiO_2 nanoparticles: strategies comparison

Authors: M. Jazmín Penelas, Galo J.A.A. Soler-Illia, Levi Valeria, Andrea V. Bordoni, Alejandro Wolosiuk

PII: S0927-7757(18)31710-2
DOI: https://doi.org/10.1016/j.colsurfa.2018.11.023
Reference: COLSUA 22993

To appear in: *Colloids and Surfaces A: Physicochem. Eng. Aspects*

Received date: 1 August 2018
Revised date: 6 November 2018
Accepted date: 10 November 2018

Please cite this article as: Penelas MJ, Soler-Illia GJAA, Valeria L, Bordoni AV, Wolosiuk A, *Click*–based thiol-ene photografting of COOH groups to SiO_2 nanoparticles: strategies comparison, *Colloids and Surfaces A: Physicochemical and Engineering Aspects* (2018), https://doi.org/10.1016/j.colsurfa.2018.11.023

This is a PDF file of an unedited manuscript that has been accepted for publication. As a service to our customers we are providing this early version of the manuscript. The manuscript will undergo copyediting, typesetting, and review of the resulting proof before it is published in its final form. Please note that during the production process errors may be discovered which could affect the content, and all legal disclaimers that apply to the journal pertain.

ACCEPTED MANUSCRIPT

Click–based thiol-ene photografting of COOH groups to SiO_2 nanoparticles: strategies comparison

Penelas[1,2], M. Jazmín, Soler-Illia[2], Galo J. A. A., Levi, Valeria[3], Bordoni[1], Andrea V., Wolosiuk[1], Alejandro

1. Gerencia Química - Centro Atómico Constituyentes – Comisión Nacional de Energía Atómica. CONICET. Av. Gral. Paz 1499, 1650, San Martín, Pcia. Buenos Aires, Argentina. E-mail: wolosiuk@cnea.gov.ar.
2. Instituto de Nanosistemas, Universidad Nacional de San Martín, Av. 25 de Mayo 1021, B1650KNA-San Martín, Buenos Aires, Argentina.
3. Universidad de Buenos Aires, Facultad de Ciencias Exactas y Naturales, Departamento de Química Biológica, Argentina- CONICET - Universidad de Buenos Aires. Instituto de Química Biológica de la Facultad de Ciencias Exactas y Naturales (IQUIBICEN), Buenos Aires. Argentina.

Graphical abstract

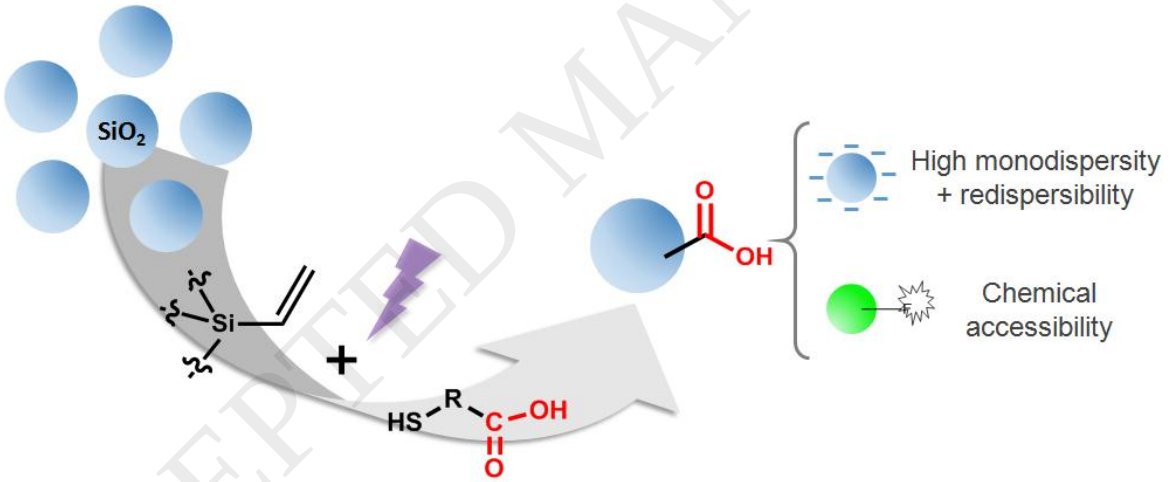

ACCEPTED MANUSCRIPT

ACCEPTED MANUSCRIPT

Abstract

We present the study of the anchoring of carboxylic groups on SiO_2 nanoparticles from different approximations based on the photochemical radical thiol-ene addition (PRTEA) reaction: a photografting approach between mercaptosuccinic acid (MSA) and vinyl-modified SiO_2 nanoparticles and the post-grafting on the surface of silica colloids of the silane precursor 2-((2-(trimethoxysilyl)ethyl)thio)succinic acid (TMSMSA), obtained from the PRTEA. These synthetic strategies were compared with a widely common derivatization methodology based on the nucleophilic attack of surface-anchored amino groups with succinic anhydride. The successful functionalization of the colloidal silica was confirmed by infrared spectroscopy (FTIR), zeta potential at different pH and contact angle measurements. We found that although these three approaches were valid for -COOH immobilization, they had a noticeable impact on the dispersability and agglomeration of the colloidal suspension at the end of the synthesis. Scanning electron microscopy, dynamic light scattering (DLS) and fluorescence correlation spectroscopy (FCS) measurements indicated that the PRTEA photografting between MSA and vinyl-modified SiO_2 resulted in highly dispersed colloidal particles. On the other hand, the presence of surface –COOH groups was highly beneficial for redispersion of the colloidal material after lyophilization or freeze-drying procedures.

Keywords: Thiol-ene addition; colloids; click-reactions; silica; carboxylic groups

1. Introduction

Organosilica hybrid nanomaterials have become an essential building block for the synthesis and design of a wide variety of platforms with chemically modified surfaces. The silica chemistry can be combined with highly tunable organic moieties, tailoring special properties for biomedical, catalysis and optical applications.[1, 2]In this context, sol-gel chemistry finds an interesting niche where technological applications require bridging polymers, metals and glasses together; from biocompatible implants to waveguiding in optical materials[3, 4]. For instance, the development of stable and non-flammable hybrid composite polymer electrolytes for Li-ion batteries relies on the mixing of composites based on poly(ethylene glycols) and organic-inorganic silica nanoparticles formed in situ [5]. Evidently, the simple synthesis of organoalkoxysilanes molecules with the general formula $R'_nSi(OR)_{4-n}$is mandatory for obtaining key intermediates in the sol-gel processing as building blocks for the chemical functionalization of SiO_2 materials.[6] In particular, immobilizing carboxylic groups on SiO_2 surfaces is a highly desirable feature as they can switch surface charges with pH in adsorption processes [7, 8], stabilize Janus-type catalytic colloids[9], improve nanoparticles stability in freeze-thaw cycles and lyophilization[10] and are long-know anchor group for protein immobilization[11]. The lack of commercial availability of carboxylic organosilanes drove several synthetic methodologies for the incorporation of COOH groups onto

ACCEPTED MANUSCRIPT

various SiO_2 surfaces either by co-condensation or postgrafting: modification of a NH_2-functionalized surface with succinic acid, grafting of an organosilane bearing an ester group that gives rise to free carboxylic moiety after a hydrolysis step, hydrolysis of the nitrile group under hard acidic conditions. [12, 13] More recently, Feinle et al. reported the use of PtO_2 as catalyst for the hydrosilylation of carbenoic acids with trialkoxysilanes[14, 15]. On the other hand, we have shown a simple approach for the synthesis of a series of organosilanes bearing deprotected carboxylic acids for a versatile functionalization of SiO_2 mesoporous particles and thin films using the *click*-based photochemical radical thiol-ene addition (PRTEA)[15-18].This reaction involves the addition of a radical thiol, $RS^{\bullet}$ to an alkene molecule (hydrothiolation) and usually requires a photoinitiator (e.g. benzophenone) for an efficient $RS^{\bullet}$ production, as schematized in Scheme 1. This reaction scheme has been successfully employed to modify transition metal oxides, polymers and metals (for more specialized reviews see refs [6, 19, 20]). The anchoring of the carboxylic group using PRTEA results highly attractive as it involves an extremely simple synthetic step that does not require organic synthesis skills or specialized equipment and attains total reactant conversion after UV irradiation.

In the present paper we explored the anchoring of carboxylic groups on SiO_2 nanoparticles from different approximations of the PRTEA reaction: a post-photografting approach between the mercaptosuccinic acid (MSA) and vinyl-modified SiO_2 nanoparticles and the post-grafting on the surface of silica colloids of the silane precursor 2-((2-(trimethoxysilyl)ethyl)thio)succinic acid (TMSMSA), obtained from the PRTEA (see Scheme 2). These approximations were compared with a widely common post-modification methodology based on the use of 3-aminopropylsilane and the posterior derivatization with succinic anhydride. Although the three approaches are valid for -COOH immobilization, they have a noticeable impact on particles dispersibility and agglomeration both of the colloidal suspension at the end of the synthesis and of the fluorescent derivatives obtained by chemical post functionalization with fluorescein, as evidenced from light scattering measurements and FCS measurements, respectively. On the other hand, an improvement was also found in the dispersibility of the –COOH functionalized NPs after being frozen or dried with respect to the unmodified SiO_2.

2. Materials and methods

2.1 Materials

Tetraethylorthosilicate (98%, TEOS), vinyltriethoxysilane (97%, VTES), vinyltrimethoxysilane (98%, VTMS), aminopropyltriethoxysilane (99%, APTES), 2-mercaptosuccinic acid (97% MSA),

ACCEPTED MANUSCRIPT

benzophenone (99%, Ph_2CO), N,N- diisopropylethylamine (99%, DIPEA), succinic anhydride (99%), 1-(3-dimethylaminopropyl)-3-ethylcarbodiimidehydrochloride (EDC), N-hydroxysuccinimide (NHS), 6-aminofluorescein hydrochloride (95%, 6 F-NH_2), 5(6)-carboxifluorescein (F-COOH) were obtained from Sigma-Aldrich. Concentrated aqueous ammonia (28%) and absolute ethanol were obtained from Biopack. Methanol (MeOH) and tetrahydrofurane (THF) were from Merck. Methanol was dried over activated MS-3 Å before used. Water used was deionized (18MΩcm^{-1}) and filtered.

2.2 Synthesis

2.2.1 Synthesis of SiO_2 NPs

Silica NPs was prepared according the Stöber method.[21] TEOS was added under vigorous stirring to a mixture containing H_2O, concentrated aqueous ammonia and absolute ethanol. Typically, the molar concentration were TEOS 0,18 M, NH_3 0,5 M and H_2O 2 M. The mixture was stirred overnight under room temperature. The resultant suspension was used without further treatment for the next steps.

2.2.2 Synthesis of SiO_2-CH=CH_2 and SiO_2-NH_2

SiO_2-CH=CH_2 nanoparticles were synthesized from the bare SiO_2 nanoparticles suspension previously obtained. The amount of VTES used in the synthesis corresponds to 50 times that required to cover the SiO_2 NP surface with a monolayer of organosilane, assuming a grafting density of 2 molecules /nm^2. In turn, the surface was calculated from the hydrodynamic diameter obtained by DLS and assuming that the density of the SiO_2 NP is 1.58 g/cm^3. The volume of VTES thus calculated was added to the SiO_2 suspension under stirring and allowed to react overnight at room temperature. The SiO_2-CH=CH_2 suspension was then distilled under vacuum using a rotary evaporator to remove ammonia and water, until suspension pH was 6-7 (it was necessary to add extra ethanol to prevent the suspension from drying out). Excess vinylsilane was removed after two cycles of centrifugation and resuspension in fresh ethanol. The final pH of the suspension was 5-6. The washed SiO_2-CH=CH_2 nanoparticles were then dispersed in ethanol, to obtain an approximately 6% w/v stock suspension. On the other hand, the SiO_2-NH_2 NP were synthesized adding APTES to a 2.5% v/v absolute ethanol solution, and then allowed to react for 5 h at room temperature according to previous works.[2] In this case, the excess of silane was removed first in two centrifugation/redispersion cycles while the remaining ammonia was removed under reduced pressure. The final concentration of these particles was 1.5 % w/v and the suspension pH was 6-7.

2.2.3 Synthesis of SiO_2-COOH derivatized nanoparticles

Photo-grafting approach (PhG-SiO_2): Carboxylic functional groups were anchored to the surface of SiO_2-CH=CH_2 NP by PRTEA. For this purpose, SiO_2-CH=CH_2 NP stock suspension was added to a ethanol solution containing MSA and Ph_2CO to reach a final composition of 1 : 1 : 0.2 in VTES

ACCEPTED MANUSCRIPT

(initially added for SiO_2-CH=CH_2 NP synthesis) : thioacid : Ph_2CO mole ratio. The final concentration of the reaction suspension was 1% w/v in SiO_2-CH=CH_2 NP. The reaction suspension was then irradiated under stirring for 17 h, using a 15W, 18"-long black-light lamp ($\lambda_{máx}$=352 nm). The product was washed with ethanol and water several times. The washed SiO_2-COOH nanoparticles were dispersed in ethanol, to reach a final concentration of the suspension of approximately 6% w/v.

Post-grafting approach (PG-SiO_2): First, 2-((2-(trimethoxysilyl)ethyl)thio)succinic acid (TMSMSA) was prepared by PRTEA as previously reported [14]**.** MSA, VTMS, Ph_2CO and methanol were mixed in a 1 : 1 : 0.15 : 11 molar ratio, representing approximately 34 monolayers. This reaction solution was irradiated in the same conditions as in photografting approach. The carboxylic-derivatized silane was later anchored to the surface of SiO_2 NP by post-grafting. For this purpose, the entire reaction volume of the photoreaction was added dropwise to a 1,5% w/v of an ethanolic suspension of SiO_2 under stirring using DIPEA as a base catalyst.[22] This suspension was allowed to react at room temperature during overnight, and finally the temperature was raised to 45 °C for 2 h. The product was decanted, washed with ethanol and water several times, centrifuged and re-suspended in ethanol.

Succinic anhydride reaction with amine derivatized approach (SA-SiO_2): For this strategy, we used the method previously used by Joselevich et al. [23] The necessary volume of the stock ethanolic solution of SiO_2-NH_2 was centrifuged and resuspended in THF by ultrasonication, to obtain a 1.25% m/V suspension. The succinic anhydride was then added with stirring and the mixture was allowed to react overnight at room temperature. The molar ratio used was 8:1 SA:APTES (initially added in the synthesis of SiO_2-NH_2 NPs). The mixture was decanted, centrifuged, and the solid obtained was washed several times with THF, ethanol, water and ethanol again.

2.2.4 Synthesis of colloidal fluorescent probes

The fluorescein derivative was immobilized on the surface of the SiO_2-COOH NP through a coupling reaction in aqueous medium between the surface -COOH and the -NH_2 group of 6-aminofluorescein (F-NH_2), according to the method previously used by Jain[2]. To this end, solutions of concentration of 1.5 mg/1 mL of EDC and NHS in water and 0.2 mg/0.2 mL of F-NH_2 in DMF were prepared. From the last solution, a 1:10 dilution in water was made, and this was used for the synthesis. To carry out the reaction, the necessary volume of the aqueous solutions of EDC, NHS and F-NH_2 was added successively to 1 mL of aqueous suspension containing 20 mg of SiO_2-COOH, in order to obtain a molar ratio –COOH : F-NH_2 : EDC : NHS of 1 : 0.01 : 0.3 : 0.3. Then, water was added to complete a final volume of 2 mL. The number of moles of -COOH was estimated from the surface of the NP calculated from its hydrodynamic diameter and SiO_2 NP density, in the same way as for the silanization functionalizations previously described, assuming

ACCEPTED MANUSCRIPT

a grafting surface density of 2 groups -COOH/nm^2. The mixture was allowed to react for 1.5 h under stirring at room temperature. To compare, using an analogous coupling methodology, carboxyfluorescein was bound to the surface of the SiO_2-NH_2 NPs. For FCS assays, a greater amount of immobilized fluorescein was required to achieve signal detection, so the synthesis was repeated using a ratio of –COOH : F-NH_2 of 1 : 1.

2.2.5 Dispersion of the nanoparticles in reconstituted suspensions

10 mg of the NP's dried under vacuum at room temperature for a week, were resuspended in 0.6 mL of mQ water, stirred with vortex, ultrasonicated for 15 minutes and then were left for 2 days. Afterwards, 30 μL of the reconstituted suspension was diluted in approximately 12 mL of ethanol, and DLS measurement was performed as described above.

2.3 Characterization of SiO_2 and surface modified SiO_2 nanoparticles

2.3.1 FTIR

Samples were prepared mixing the NP's previously dried under vacuum at room temperature for at least 4 days with KBr, until reach a final composition of 3% w/w. The mixture was then ground and dried 1 h at 130 °C before measure. Fourier Transform Infrared Spectroscopy measurements were performed with a Nicolet Magna 560 instrument, equipped with liquid N_2 cooled MCT-A detector in DRIFT mode.

2.3.2 Zeta potential

Samples were prepared by adjusting the pH by adding small aliquots of HCl and NaOH solutions to SiO_2 and modified SiO_2 NP suspensions of approximate concentration 0.015% w/v in aqueous KCl 10 mM. The pH values were measured using a pH-meter Metrohm 691. The measurements were performed in duplicate in a Zetasizer 2000 (Malvern Instruments Ltd.).

2.3.3 Thermogravimetric Analysis (TGA)

The surface grafting density of functional chemical groups (δ, number of chemical functional groups / nm^2) was calculated using the Equation 1 from the mass loss obtained by TGA and NPs parameters.[24] Thermograms were first normalized respect to their initial mass and we assumed that before 200°C all mass losses where due to water removal. In Equation 1, m_{org} is the final mass difference; m_{inorg} is the remaining inorganic mass, S_{NP}, V_{NP} and ρ correspond to the surface, volume and density of the SiO_2 NPs from geometric estimations, M_{org} is the molecular weight of the incorporated organic group and N_A is the Avogadro's number. For the nanoparticle density, ρ, we assumed a value of 1,58 g/cm^3 from literature.[25]

ACCEPTED MANUSCRIPT

$$\delta_{exp} = \frac{\left(\frac{m_{org}}{m_{inorg}}\right)\rho V_{NP} N_A}{M_{org} S_{NP}} \quad \textbf{(1)}$$

TGA was performed in air at a heating rate of 10 °C/min from room temperature to 650 ° C (TA Instruments, SDT Q600).

2.3.4 Contact angle

The measurement was performed on colloidal films prepared from 6% w/v ethanol suspension of the NP's. In order to obtain them, square pieces of glass slides were prepared first immersed them in piranha solution for 15 minutes, then washed with plenty of water, and dried at 130 °C. Afterward, 100 µL of the suspensions, previously ultrasonicated for 15 minutes, was spin coated at approximately 8000 rpm onto the clean glass slides and dried al 130 °C for 10 minutes; this last step was repeated 5 times. Just before measure, the colloidal films were dried at 130 °C for 1 h and let them cool in a desiccator. The contact angle was determined by the sessile drop method, using an automated Ramé-Hart Model 290 F4 Series goniometer. The value was obtained from the analysis with the Software Drop Image Advanced v.2.5 of a digital photograph acquired immediately after depositing the drop on the film as the slope of the contour of the drop at the point of contact of the three phases. The contact angle values reported correspond to the average between the right and left angle of the drop for seven drops deposited in different areas of the film. For each sample of NP's, the films were prepared and measured in duplicate. All the measurements were carried out under environmental conditions.

2.3.5 Dynamic light scattering

Samples were prepared by diluting a 50 µL aliquot of the NP suspension in approximately 12 mL of ethanol. After ultrasonication for a few minutes, the sample was measured in a BI-200SM Goniometer Ver. 2.0 (Brookhaven Instrument Corp.) scanning the range of 30-150° every 10° (λ=637nm) at 25 °C. Hydrodynamic diameter of the NP was calculated using the Stokes-Einstein equation from the cumulant analysis from Brookhaven Instruments built-in software package. Polydispersity Index (PDI) was calculated from the cumulants analysis and is dimensionless value of the broadness of the particle size distribution.

2.3.6 Scanning electron microscopy

Samples for imaging were prepared depositing a drop of a diluted suspension of the NP in ethanol on a small piece of Si wafer supported on a standard aluminum 12.7 mm pin stub covered with

ACCEPTED MANUSCRIPT

self-adhesive carbon tape. Field emission scanning electron microscopy (FESEM) images were taken with a Carl Zeiss NTS - SUPRA 40.

2.3.7 Fluorescence and absorbance spectra

Fluorescence emission spectra were recorded using a PTI QuantaMaster™ 4 CW fluorometer, equipped with a xenon short-arc lamp UXL-75XE in a 1x1 cm quartz cell, from an aqueous suspension of 0.1 mg/mL concentration in NP, brought to pH 8 with NaOH solution. The excitation wavelength was 470 nm, and the emitted light was collected at 90° with respect to the excitation beam. The anisotropy of the emission, r, was determined using DMF as the suspension solvent for suppress the effect of dispersion on the obtained spectra. Spectra were taken by exciting the wavelength of the emission maximum, using one polarizer for the excitation and another for the emission, in the four possible configurations between the vertical and horizontal orientations. r was subsequently calculated according to the formula:

$$r = \frac{I_{VV} - G.I_{VH}}{I_{VV} + 2G.I_{VH}} \quad \textbf{(2)}$$

Where

$$G = \frac{I_{HV}}{I_{HH}} \quad \textbf{(3)}$$

In parallel, the absorbance spectrum of each sample was measured in a Cary 50 Conc UV–Vis Spectrophotometer (Varian).

2.3.8 Fluorescence correlation spectroscopy

FCS measurements were performed in an FV1000 confocal microscope with the detector set in photon counting mode. The excitation laser was a multi-line Ar laser tuned at 488 nm (average power at the sample, 300 nW). The laser light was reflected by a dichroic mirror (DM 405/488) and focused through an Olympus UPlanSApo 60× oil immersion objective (NA = 1.35) onto the sample. Fluorescence was collected in the range 500–600 nm at a frequency of 100000 Hz during 90 s. The intensity trace was used to calculate the autocorrelation function as:

$$G(\tau) = \frac{\langle \delta I(t) \cdot \delta I(t+\tau) \rangle}{\langle I(t) \rangle^2} \quad \textbf{(4)}$$

where I(t) represents the fluorescence intensity at time t, the brackets indicate average values over the time-course of the experiment and δI(t)=I(t)-<I(t)> represents the fluorescence fluctuation. The autocorrelation data was fitted with Eq (5) that assumes 3D free diffusion[26]:

ACCEPTED MANUSCRIPT

$$G(\tau) = G_o \left(1 + \frac{\tau}{\tau_D}\right)^{-1} \left(1 + \frac{\tau}{\omega^2 \tau_D}\right)^{-1/2} \quad \textbf{(5)}$$

where G_o is the correlation function amplitude and τ_D, the characteristic diffusion time, can be used to estimate the diffusion coefficient of the probe [27]:

$$D = \frac{\omega_0^2}{4\tau_D} \quad \textbf{(6)}$$

where ω_o is the axial waist of the confocal observation volume (0.26 $\pm$ 0.01 μm, N =5) and was estimated using a reference solution of Rhodamine B in a 50% glycerol solution (D = 73 $\mu m^2/s$). From the Stokes - Einstein relationship, $D = \frac{k_B T}{6\eta D_H}$ we obtain the hydrodynamic diameter (D_H) of the particles. Recently, for colloids and nanoparticles that have diameters that are comparable in size to the confocal volume a correction is needed [28, 29]:

$$\frac{\tau_c}{\tau_0} = 1 + k\left(\frac{a^2}{(\omega_0/2)^2}\right) \quad \textbf{(7)}$$

where τ_c is the measured correlation time, τ_0 is the correlation time of a colloidal particle of the same radius but fluorescently labelled only in the center, *a* is hydrodynamic radius of the particle and *k* is a dimensionless constant for different labelling configurations. In our case, for a surface anchored dye *k*=0.42.

Typically, between 7 to 30 independent FCS measurements were run for each experimental condition.

3. Results and discussion

3.1 COOH anchoring schemes to SiO_2 NP

Scheme 2 shows the different synthetic routes used to obtain surface functionalized carboxylic SiO_2 nanoparticles. The starting silica spherical nanoparticles were obtained employing the Stöber-Fink-Bohn method. [21] After the synthesis, its surface can be easily modified with organoalkoxysilanes for further bridging of inorganic/organic components [30] with the following synthetic schemes:

a) In the photo-grafting approach, the SiO_2 NP surface was modified with vinyl groups by one-pot silanization with VTES. Excess vinylsilane is washed by centrifugation and resuspension in ethanol; the resulting colloidal suspension is used directly for the PRTEA-*click* reaction with MSA.

ACCEPTED MANUSCRIPT

b) In the post- grafting approach, the PRTEA-*click* reaction is carried out in solution first between the MSA and the VTMS. Subsequently, the organoalkoxysilane obtained was used as is for the surface modification of the SiO_2 NPs.
c) Finally, the obtained -COOH SiO_2 NP were compared with a relatively common and widespread synthetic route based on the nucleophilic attack of anchored amino groups to a succinic anhydride (SA) molecule.[23] The first step was the one-pot silanization with APTES of the bare silica NPs that later react with SA resulting in a surface carboxylic terminal group.

3.2 SiO_2 NP physicochemical characterization

3.2.1 FTIR, zeta potential, contact angle measurements

Figure 1 compares the FTIR spectra of bare SiO_2 nanoparticles, PRTEA MSA photografted SiO_2 nanoparticles (PhG-SiO_2), post-grafted of a PRTEA MSA silane precursor (PG-SiO_2) and the derivatization reaction of amine modified SiO_2 NP with succinic anhydride (SA-SiO_2). When a COOH is present, we observe the C=O stretching vibration at ~1725 cm^{-1}, in agreement with previous reports from our group [17, 18, 31]. All the samples show the typical broad band originated in the OH stretching of hydrogen bonded water molecules to the surface silanol and anchored carboxylic groups between 3800 – 3200 cm^{-1} (Figure ESI 3) and the band at 1630 cm^{-1} due to the scissor bending vibration of the OH groups. Similar spectra have been obtained for the PRTEA photografted reaction between other thioacids such as mercaptoacetic acid (MAA), mercaptopropionic (MPA) and mercaptoundecanoic acid (MUDA) (Figure ESI 1.(a)). Other bands due to the anchored functional groups in the 1200 – 800 cm^{-1} region are completely masked by the strong Si-O-Si vibrations. In the case of the SA-SiO_2 NPs obtained by derivatization of the amino group, the amide N-H bending generates a band at 1556 cm^{-1}. In all the spectra, signals from the stretching and deformation of the C-H bond of alkyl residues are identifiable, especially in the PG- and SA-SiO_2 spectra, although they are also present in the unmodified SiO_2 due to the presence of partially hydrolyzed TEOS groups from the synthesis by the Stöber method [32].

Figure 1b shows the zeta potential values at pH 3 and 5 of the SiO_2 NP, its derivatives functionalized with the intermediate groups and their carboxylated products. In the case of SiO_2-$CH{=}CH_2$ NP, in which the surface silanol groups were partially replaced by the non-hydrolysable vinyl organic functional group, a shift is observed towards higher pHs of the isoelectric point and, in general, less negative zeta potential values than in the case of unmodified SiO_2. After the addition of the MSA to the SiO_2-$CH{=}CH_2$ nanoparticles by the PRTEA reaction, the zeta potential values are markedly more negative than those of SiO_2 at both pHs, indicating the immobilization of negatively charged ionizable groups. This trend is consistent with COOH deprotonation on the

ACCEPTED MANUSCRIPT

particle surface in addition to the presence of isolated Si-OH groups [65]. A similar behaviour has been observed in the case of the other photographed thioacids (Figure ESI 1(b)). Aminated SiO_2 particles [33], on the other hand, show positive values in the pH range explored; nonetheless, an inversion of the surface charge is observed when reaction with succinic anhydride results in COOH groups[34]. The derivatized product with succinic anhydride, unlike the PhG-SiO_2NPs, has a positive charge at pH 3, and recently acquires negative values at higher pH, which suggests that unmodified amino groups remain on its surface. Photografted PRTEA chemical surface modification can be easily correlated with the hydrophilicity changes of the surface chemical groups associated with each reaction step in this series as is evident in the contact angle values of the colloidal films corresponding to each nanoparticle, as presented in Figure 1c. Moreover, we obtain similar contact angles and zeta potential behavior for the SiO_2 NP photographted with other thioacids as MAA, MPA and MUDA (Figures ESI 1 (c) and 2).

The previous observations agree very well with thermograms of the different modified SiO_2 NPs, shown in Table 1. If we observe the grafting density of the SA-SiO_2, it is clear that the SA molecules intoduced do not modify completely the anchored NH_2 groups. These moieties reveal themselves when the zeta potential is analyzed in solutions of low pH. On the other situations, PG-SiO_2 and PhG-SiO_2, we obtained similar grafting COOH densities. Moreover, since MSA carries two COOH groups we should have expected a theoretical 2:1 ratio with the vynil-modified surface; however, surface steric limitations must limit the number of COOH groups.

3.2.2 DLS

DLS provides valuable information of the level of aggregation and interaction between suspended particles in solution. Table 2 shows the ratio of the hydrodynamic diameter values obtained by DLS between the functionalized particles and the respective unmodified SiO_2 NPs precursors. In the case of PhG-SiO_2 NPs, we observed that the original hydrodynamic diameter is conserved throughout all the synthesis steps: vinyl surface functionalization and photo-grafting of the MSA molecule. In this context, we may remind the reader that the post-grafting of thioacids to anchored vinyl groups on the SiO_2 particle has been referred as an "ene-thiol" approach. [35] In this case, the photogenerated $RS^{\bullet}$ thiols attack the surface anchored vinyl groups forming a thioether bond. On the other hand, when surface bound thiols react with vinyl compounds in solution the “thiol-ene” reaction may result in an undesired surface polymerization. [36] Thus, it is apparent after observing Table 2 that the particles remain dispersed in solution after the “ene-thiol” PRTEA. Moreover, the polidispersity index (PDI), which is a measure of the sample monodispersity, shows no appreciable difference after surface modification (PDI_{SiO_2}=0.030, $PDI_{SiO_2-CH=CH_2}$=0.032 and $PDI_{PhG-SiO_2}$=0.048). This result can also be explained taking into

ACCEPTED MANUSCRIPT

account that the approach used for the synthesis proceeds entirely in ethanol solution, solvent whereby both bare and modified SiO_2 have great affinity, involves few separation steps and those that do not cause destabilization of the colloidal system.

When we analyze the functionalization by post-grafting of the carboxyl-derivatized silane, there is a slight increase in the apparent hydrodynamic radius from DLS measurements and a slight tendency towards greater polydispersity (PDI_{SiO_2}=0.085 and PDI_{PG-SiO_2}=0.122). However, the degree of final monodispersion can be considered satisfactory and is also correlated with the synthesis methodology.

On the other hand, the most notable contrast occurs in the case of the derivatization of surface bound amino groups. For this system we observe increased hydrodynamic diameters right after silanization with APTES, evidenced by a ratio very far from 1 and a high deviation diameter standard, due to the presence of polydispersed aggregates. This situation is also observed in the PDI values ($PDI_{SiO_2-NH_2}$ =0.147 vs PDI_{SiO_2}=0.085). After derivatizing the amino groups with succinic anhydride, the starting hydrodynamic diameters are hardly recovered (PDI_{SA-SiO_2}=0,129). Colloidal aggregation of SiO_2 NP after APTES surface modification is commonplace and has been observed by various groups [37, 38]. This can be attributed to the fact that as -NH_2 groups are anchored to the surface there is a slow decrease in the isoelectric point of the SiO_2 surface due to silanol replacement. In other words, nanoparticle and colloidal stability are compromised because the silanol moieties are replaced with positively charged NH_4^+ or uncharged NH_3. Other sources of surface potential change have been recognized: formation of "clusters" of amine groups in hydrophobic coating solutions [39] and NH_3^+ functions transferring a proton to neighboring Si-O^- surface groups in an irreversibly manner[40]. Because of the aforementioned conditions, reversible and irreversible aggregation are usually observed as soon APTES is introduced in the alcosol medium for a "one-pot" approach. Common solutions to this problem relied on membrane filtration[41], centrifugation/redispersion cycles[37] and sonication[42]. Despite these obvious differences that can be found for particle sizing, PDI also gives a clear indication of the different dispersability of the SiO_2-COOH particles in aqueous solutions.

3.2.3 FESEM images

Figure 2a shows typical FESEM image of a batch of synthesized SiO_2 spherical nanoparticles with a diameter of 56 ± 6 nm. It should be noted that the characterization of the SiO_2 NP by DLS yielded a value for its hydrodynamic diameter of 72 ±3 nm. Nanoparticle and colloid dimensions differences observed between electron microscopy and dynamic light scattering techniques are

ACCEPTED MANUSCRIPT

relatively common and can be attributed to the particle composition (e.g. metallic, oxide, polymeric) that ultimately defines the surface interface chemistry [43]. Recently, Škvarla and coworkers, using atomic force microscopy, have proposed the existence of an elastic gel layer on the SiO_2 colloidal surface that results in apparent "bigger" objects when in aqueous solutions[44]. At first glance, there are no differences neither in particle shape nor size after functionalization. Evaluating dispersibility of nanoparticle objects only from electron microscopy images is difficult due to capillary forces during specimen drying on supporting substrates; nevertheless, in the SEM images of SiO_2-NH_2 and PG-SiO_2 NPs it can be seen how the former are mostly in the form of agglomerates, while the latter are more dispersed and even many are isolated, showing a correlation with DLS measurements in aqueous suspensions.

In summary, the three synthetic approaches presented are valid for -COOH immobilization but have substantial differences regarding particle dispersibility and agglomeration of the colloidal suspension during the synthesis. PhG-SiO_2 showed little or no aggregation at all during the chemical modification steps and will prove to be highly important as we will see below.

3.2.4 Lyophilization and reconstitution of COOH- modified SiO_2 NP

Recently, lyophilization of nanoparticles has gained considerable interest for pharmacological and nanobiotechnological applications, in order to preserve their chemical and physical integrity [45]. For instance, mercaptoacetic functionalized Au nanoparticles have shown exceptional stability in lyophilization procedures[10]. Given that the PhG-SiO_2 NPs exhibited remarkable dispersibility properties, we analyzed reconstituted suspensions from the unmodified SiO_2 and PhG-SiO_2 NPs after freezing and drying treatments, two instances related to the lyophilization process.

We observed that the suspensions of bare SiO_2 NPs reconstituted from frozen solutions and those dried in vacuum at room temperature for a week, in both ethanol and water, have higher mean D_H compared to the initial suspensions. Besides, standard deviations and average polydispersity increase simultaneously ($PDI_{SiO_2,frozen}$ =0,120 and $PDI_{SiO_2,dried} = 0{,}144$ vs. $PDI_{SiO_2,initial}$=0.037), which we attibute to the presence of a fraction of SiO_2 NPs that aggregate in an irreversibly manner. Hydrogen bonding interactions are established between the nanoparticles through the surface silanol groups as the solution freezes. Moreover, these interactions are promoted both by the increase in local concentration (the formation of ice excludes solutes/colloids), the mechanical stress derived from crystallized water and the dehydration of the surface of the particles that take place during both treatments.[46] In contrast, freezing dry PhG-SiO_2 NPs maintains both narrow diameter distribution and average polydispersity similar to the respective initial suspensions ($PDI_{SiO_2-COOH,frozen}$ =0,082 and $PDI_{SiO_2-COOH,dried} = 0{,}024$ vs. $PDI_{SiO_2-COOH,initial}$=0.048). In this case, the presence of

ACCEPTED MANUSCRIPT

ionizable moieties keeps the particles dispersed by electrostatic repulsion, contributing to the stability of the colloidal suspension.[47]

3.2.5 Chemical post-functionalization of COOH-modified SiO_2 NP: Fluorescein labelling

We have shown in previous works that the immobilized COOH groups within porous SiO_2 frameworks are chemically accessible for acid-base reactions and metal and lanthanide adsorption [17, 18, 31]. In this context, we tested the anchoring of a fluorescent dye as fluorescein with surface complementary dangling group amino fluorescein using a carbodiimide approach.

Figure 3 shows the fluorescence spectrum of the PhG-SiO_2, after being modified with aminofluorescein according to Scheme 3, with a maximum emission at 517 nm. Similar spectra have been obtained for the other fluorescent derivatives from the carboxylic NPs; small differences in peak emission (~5 nm) respect to the free dye can be attributed to the change of photophysical parameters and have been observed in surface immobilized dyes (Figure ESI 5(a)).[48, 49] When the coupling reagents EDC and NHS are not present there is no fluorescence signal, pointing that the immobilization of fluorescein does not take place and we can rule out adsorption of the dye on the SiO_2 surface. Interestingly, the emission band of fluorescein anchored to the nanoparticle presents a remarkable increase in intensity compared to that corresponding to free dye at the same concentration. This was previously reported and attributed to the suppression of the self-quenching effect generated by the free electron pair of the amino group on the fluorophore when it becomes involved in a covalent bond, which results in an increase in quantum fluorescence yield[50]. In addition, the immobilization of fluorescein on the surface of the nanoparticle is verified from fluorescence anisotropy experiments where we obtain an anisotropy of 0.2 at the wavelength of the emission maximum, close to the theoretical value of 0.3 (Figure 3 Inset). [51]

3.2.6 Fluorescence correlation spectroscopy

The anchoring of fluorescent dyes to nanoparticles and colloids is an essential step for the design of cellular probes and sensors. FCS analysis of monodispersed luminescent probes offers a valuable tool for tracking molecular and biomolecular events. In this context, we studied the performance of the fluorescent derivatized SiO_2-COOH NPs for FCS techniques. Figure 4 shows the normalized fluorescence intensity fluctuations of the PhG-SiO_2 and PG-SiO_2 NPs. It is evident that only the aqueous suspensions of the F-PhG-SiO_2 probes derived from the SiO_2-COOH obtained via PRTEA produced a relatively monodisperse population that gives an almost random fluorescence intensity fluctuation (Figure 4a). On the other hand, F-PG-SiO_2 NPs show an irregular intensity fluctuation trace with the presence of spikes due to the presence of aggregates (Figure 4b). These results are in excelent agreement with the DLS results observed previously. Moreover,

ACCEPTED MANUSCRIPT

carboxyfluorescein anchored to APTES derivatized SiO_2 NPs and aminofluorescein bound to SA-SiO_2 resulted in highly polydisperse samples for FCS and could not be analyzed with this technique (not shown), as already observed with DLS. Figure 5 shows a typical FCS autocorrelation function *G(t)* for PhG-SiO_2 NPs fitted to Equation 5. The hydrodynamic diameters obtained from FCS measurements resulted slightly higher than the values obtained from DLS measurements, as summarized in Table 4. However, when we corrected the measured correlation time τ_c according to Equation 7 using the hydrodynamic radius obtained from DLS measurements, we observed that for the F-PhG-SiO_2 NPs this relation is approximately equal, suggesting a negligible aggregation of the F-PhG-SiO_2 NPs. In summary, the PRTEA reaction on SiO_2 surfaces is an attractive approach for introducing COOH groups on colloidal surfaces, avoiding aggregation issues related to post-modification of amino groups anchored on SiO_2 surfaces.

4. Conclusions

Surface carboxylic modified SiO_2 colloids were obtained from three different synthetic strategies: i) photochemical thiol-ene *click* reaction on vinyl-modified SiO_2 NP, ii) post-grafting of a carboxyl-modified alkoxysilane using PRTEA and iii) a traditional synthetic approach based on post-functionalization of amino-anchored groups. The methods employed showed remarkable differences between them in terms of aggregation, surface charge and redispersibility. Although all methods proved to functionalize successfully the SiO_2 surface with carboxylic groups, as evidenced from FTIR and TGA, colloidal stability and aggregation can be compromised along the surface modification process. This aspect is of uttermost importance if nanoparticle probes are designed to follow aggregation/adsorption processes or will work as luminescent probes. Nanoparticle surface chemistry determines the interaction of NPs with other biomolecules and their biological fate (e.g. protein corona formation).[52] In this context, PRTEA on vinyl-SiO_2 nanoparticles avoids the formation of agglomerates during surface modification, a phenomenon typically found when dealing with aminated surfaces.

Ackowledgements

We thank Dr. Martín Mirenda and Mr. Nicolás Krimer for assistance with fluorescence and anisotropy measurements. A. V. B., V.L, G.J.A.A.S.I and A.W. are research staff from CONICET. Funding was provided by the following grants: ANPCyT (PICT 2015-0351 to A.W., PICT 2015-3526 to G.J.A.A.S.I, PICT 2014-3687 to G.J.A.A.S.I, PICT 2015-0370 to V.L., UBACyT (20020150100122BA to V.L.) and CONICET (PIP11220130100121CO to V.L.).

References

ACCEPTED MANUSCRIPT

[1] J.G. Croissant, X. Cattoën, J.O. Durand, M. Wong Chi Man, N.M. Khashab, Organosilica hybrid nanomaterials with a high organic content: syntheses and applications of silsesquioxanes, Nanoscale 8(48) (2016) 19945-19972.
[2] Y. Toum Terrones, F. Coluccio Leskow, A.V. Bordoni, S.L. Acebedo, C.C. Spagnuolo, A. Wolosiuk, A silica supported tricarbocyanine based pH nanosensor with a large Stokes shift and a near infrared fluorescence response: Performance in vitro and in live cells, J. Mater. Chem. B 5(22) (2017) 4031-4034.
[3] M.A. Aegerter, M. Mennig, Sol-Gel Technologies for Glass Producers and Users, Springer US2004.
[4] L. Klein, M. Aparicio, A. Jitianu, Handbook of Sol-Gel Science and Technology: Processing, Characterization and Applications, Springer International Publishing2018.
[5] T. Blensdorf, A. Joenathan, M. Hunt, U. Werner-Zwanziger, B.D. Stein, W.E. Mahmoud, A.A. Al-Ghamdi, J. Carini, L.M. Bronstein, Hybrid composite polymer electrolytes: ionic liquids as a magic bullet for the poly(ethylene glycol)-silica network, Journal of Materials Chemistry A 5(7) (2017) 3493-3502.
[6] A.V. Bordoni, M.V. Lombardo, A. Wolosiuk, Photochemical radical thiol-ene click-based methodologies for silica and transition metal oxides materials chemical modification: A mini-review, RSC Advances 6(81) (2016) 77410-77426.
[7] E.D. Steinle, D.T. Mitchell, M. Wirtz, S.B. Lee, V.Y. Young, C.R. Martin, Ion channel mimetic micropore and nanotube membrane sensors, Anal. Chem. 74(10) (2002) 2416-2422.
[8] L. Xu, N. Liu, Y. Cao, F. Lu, Y. Chen, X. Zhang, L. Feng, Y. Wei, Mercury ion responsive wettability and oil/water separation, ACS Appl. Mater. Interfaces 6(16) (2014) 13324-13329.
[9] A. Kirillova, C. Schliebe, G. Stoychev, A. Jakob, H. Lang, A. Synytska, Hybrid Hairy Janus Particles Decorated with Metallic Nanoparticles for Catalytic Applications, ACS Appl. Mater. Interfaces 7(38) (2015) 21224-21225.
[10] A.M. Alkilany, S.R. Abulateefeh, K.K. Mills, A.I. Bani Yaseen, M.A. Hamaly, H.S. Alkhatib, K.M. Aiedeh, J.W. Stone, Colloidal stability of citrate and mercaptoacetic acid capped gold nanoparticles upon lyophilization: Effect of capping ligand attachment and type of cryoprotectants, Langmuir 30(46) (2014) 13799-13808.
[11] G.T. Hermanson, Chapter 3 - The Reactions of Bioconjugation, in: G.T. Hermanson (Ed.), Bioconjugate Techniques (Third Edition), Academic Press, Boston, 2013, pp. 229-258.
[12] L. Han, O. Terasaki, S. Che, Carboxylic group functionalized ordered mesoporous silicas, J. Mater. Chem. 21(30) (2011) 11033-11039.
[13] C. Beck, W. Härtl, R. Hempelmann, Covalent surface functionalization and self-organization of silica nanoparticles, Angew. Chem. Int. Ed. 38(9) (1999) 1297-1300.
[14] A. Feinle, S. Flaig, M. Puchberger, U. Schubert, N. Hüsing, Stable carboxylic acid derivatized alkoxy silanes, Chemical Communications 51(12) (2015) 2339-2341.
[15] A. Feinle, F. Leichtfried, S. Straßer, N. Hüsing, Carboxylic acid-functionalized porous silica particles by a co-condensation approach, J Sol Gel Sci Technol 81(1) (2017) 138-146.
[16] A.K. Tucker-Schwartz, R.A. Farrell, R.L. Garrell, Thiol - Ene click reaction as a general route to functional trialkoxysilanes for surface coating applications, J. Am. Chem. Soc. 133(29) (2011) 11026-11029.
[17] A.V. Bordoni, M.V. Lombardo, A.E. Regazzoni, G.J.A.A. Soler-Illia, A. Wolosiuk, Simple thiol-ene click chemistry modification of SBA-15 silica pores with carboxylic acids, Journal of Colloid and Interface Science 450 (2015) 316-324.
[18] M.V. Lombardo, M. Mirenda, A.V. Bordoni, A. Wolosiuk, A.E. Regazzoni, Chemisorption of lanthanide ions on succinate-functionalized mesoporous silica: An in situ characterization by fluorescence, Journal of Colloid and Interface Science 507 (2017) 139-144.

ACCEPTED MANUSCRIPT

[19] A.B. Lowe, Thiol-ene "click" reactions and recent applications in polymer and materials synthesis: A first update, Polym. Chem. 5(17) (2014) 4820-4870.
[20] J. Escorihuela, A.T.M. Marcelis, H. Zuilhof, Metal-Free Click Chemistry Reactions on Surfaces, Adv. Mater. Interfaces 2(13) (2015).
[21] W. Stöber, A. Fink, E. Bohn, J. Colloid Interface Sci. 26 (1968) 6269.
[22] P. Van Der Voort, E.F. Vansant, Silylation of the silica surface. A review, J. LIQ. CHROMATOGR. RELAT. TECHNOL. 19(17-18) (1996) 2723-2752.
[23] M. Joselevich, F.J. Williams, Synthesis and characterization of diazonium functionalized nanoparticles for deposition on metal surfaces, Langmuir 24(20) (2008) 11711-11717.
[24] J. Chen, M. Liu, C. Chen, H. Gong, C. Gao, Synthesis and characterization of silica nanoparticles with well-defined thermoresponsive PNIPAM via a combination of RAFT and click chemistry, ACS Appl. Mater. Interfaces 3(8) (2011) 3215-3223.
[25] V.M. Masalov, N.S. Sukhinina, E.A. Kudrenko, G.A. Emelchenko, Mechanism of formation and nanostructure of Stöber silica particles, Nanotechnology 22(27) (2011).
[26] E.L. Elson, Fluorescence correlation spectroscopy: Past, present, future, Biophys. J. 101(12) (2011) 2855-2870.
[27] E.L. Elson, Brief introduction to fluorescence correlation spectroscopy, Methods Enzymol 518 (2013) 11-41.
[28] J. Gapinski, M. Jarzębski, J. Buitenhuis, T. Deptula, J. Mazuryk, A. Patkowski, Structure and Dimensions of Core-Shell Nanoparticles Comparable to the Confocal Volume Studied by Means of Fluorescence Correlation Spectroscopy, Langmuir 32(10) (2016) 2482-2491.
[29] M. Jarzębski, T. Śliwa, B. Peplińska, J. Jakubowicz, R. Kuzioła, J. Kościński, T. Białopiotrowicz, J. Gapiński, Submicron sized fluorescent silica particles characterization, Nucl Instrum Methods Phys Res Sect B 411 (2017) 78-84.
[30] J.W. Park, Y.J. Park, C.H. Jun, Post-grafting of silica surfaces with pre-functionalized organosilanes: New synthetic equivalents of conventional trialkoxysilanes, Chemical Communications 47(17) (2011) 4860-4871.
[31] A. Escobar, L. Yate, M. Grzelczak, H. Amenitsch, S.E. Moya, A.V. Bordoni, P.C. Angelomé, One-Step Synthesis of Mesoporous Silica Thin Films Containing Available COOH Groups, ACS Omega 2(8) (2017) 4548-4555.
[32] A. van Blaaderen, A.P.M. Kentgens, Particle morphology and chemical microstructure of colloidal silica spheres made from alkoxysilanes, J Non Cryst Solids 149(3) (1992) 161-178.
[33] E. Soto-Cantu, R. Cueto, J. Koch, P.S. Russo, Synthesis and rapid characterization of amine-functionalized silica, Langmuir 28(13) (2012) 5562-5569.
[34] B.C. Ong, Y.K. Leong, S.B. Chen, Interparticle forces in spherical monodispersed silica dispersions: Effects of branched polyethylenimine and molecular weight, Journal of Colloid and Interface Science 337(1) (2009) 24-31.
[35] A. Marechal, A. Laaniste, R. El-Debs, V. Dugas, C. Demesmay, Versatile ene-thiol photoclick reaction for preparation of multimodal monolithic silica capillary columns, J. Chromatogr. A 1365 (2014) 140-147.
[36] A. Laaniste, A. Marechal, R. El-Debs, J. Randon, V. Dugas, C. Demesmay, "Thiol-ene" photoclick chemistry as a rapid and localizable functionalization pathway for silica capillary monolithic columns, J. Chromatogr. A 1355 (2014) 296-300.
[37] A. van Blaaderen, A. Vrij, Synthesis and Characterization of Colloidal Dispersions of Fluorescent, Monodisperse Silica Spheres, Langmuir 8(12) (1992) 2921-2931.
[38] M. Pálmai, L.N. Nagy, J. Mihály, Z. Varga, G. Tárkányi, R. Mizsei, I.C. Szigyártó, T. Kiss, T. Kremmer, A. Bóta, Preparation, purification, and characterization of aminopropyl-functionalized silica sol, Journal of Colloid and Interface Science 390(1) (2013) 34-40.

ACCEPTED MANUSCRIPT

[39] J.C. Hicks, R. Dabestani, A.C. Buchanan Iii, C.W. Jones, Spacing and site isolation of amine groups in 3-aminopropyl-grafted silica materials: The role of protecting groups, Chem. Mater. 18(21) (2006) 5022-5032.
[40] A. Calvo, P.C. Angelomé, V.M. Sánchez, D.A. Scherlis, F.J. Williams, G.J.A.A. Soler-Illia, Mesoporous aminopropyl-functionalized hybrid thin films with modulable surface and environment-responsive behavior, Chem. Mater. 20(14) (2008) 4661-4668.
[41] K. Natte, T. Behnke, G. Orts-Gil, C. Würth, J.F. Friedrich, W. Österle, U. Resch-Genge, Synthesis and characterisation of highly fluorescent core-shell nanoparticles based on Alexa dyes, J. Nanopart. Res. 14(2) (2012).
[42] I.A. Rahman, M. Jafarzadeh, C.S. Sipaut, Synthesis of organo-functionalized nanosilica via a co-condensation modification using γ-aminopropyltriethoxysilane (APTES), Ceram Int 35(5) (2009) 1883-1888.
[43] P. Eaton, P. Quaresma, C. Soares, C. Neves, M.P. de Almeida, E. Pereira, P. West, A direct comparison of experimental methods to measure dimensions of synthetic nanoparticles, Ultramicroscopy 182 (2017) 179-190.
[44] J. Škvarla, J. Škvarla, An identification of the soft polyelectrolyte gel-like layer on silica colloids using atomic force and electron microscopy, Ultramicroscopy 181 (2017) 97-106.
[45] A.S. Picco, L.F. Ferreira, M.S. Liberato, G.B. Mondo, M.B. Cardoso, Freeze-drying of silica nanoparticles: redispersibility toward nanomedicine applications, Nanomedicine 13(2) (2017) 179-190.
[46] W. Abdelwahed, G. Degobert, S. Stainmesse, H. Fessi, Freeze-drying of nanoparticles: Formulation, process and storage considerations, Adv. Drug Deliv. Rev. 58(15) (2006) 1688-1713.
[47] M. Liong, J. Lu, M. Kovochich, T. Xia, S.G. Ruehm, A.E. Nel, F. Tamanoi, J.I. Zink, Multifunctional inorganic nanoparticles for imaging, targeting, and drug delivery, ACS Nano 2(5) (2008) 889-896.
[48] S.G. López, G. Worringer, H.B. Rodríguez, E. San Román, Trapping of Rhodamine 6G excitation energy on cellulose microparticles, Physical Chemistry Chemical Physics 12(9) (2010) 2246-2253.
[49] Y.E. Litman, H.B. Rodríguez, S.E. Braslavsky, E. San Román, Photophysics of Xanthene Dyes at High Concentrations in Solid Environments: Charge Transfer Assisted Triplet Formation, Photochemistry and Photobiology 94(5) (2018) 865-874.
[50] N.O. McHedlov-Petrossyan, T.A. Cheipesh, A.D. Roshal, A.O. Doroshenko, N.A. Vodolazkaya, Fluorescence of aminofluoresceins as an indicative process allowing one to distinguish between micelles of cationic surfactants and micelle-like aggregates, Methods Appl. Fluoresc. 4(3) (2016).
[51] G. Hungerford, J. Benesch, J.F. Mano, R.L. Reis, Effect of the labelling ratio on the photophysics of fluorescein isothiocyanate (FITC) conjugated to bovine serum albumin, Photochem. Photobiol. Sci. 6(2) (2007) 152-158.
[52] A. Silvestri, D. Di Silvio, I. Llarena, R.A. Murray, M. Marelli, L. Lay, L. Polito, S.E. Moya, Influence of surface coating on the intracellular behaviour of gold nanoparticles: A fluorescence correlation spectroscopy study, Nanoscale 9(38) (2017) 14730-14739.

ACCEPTED MANUSCRIPT

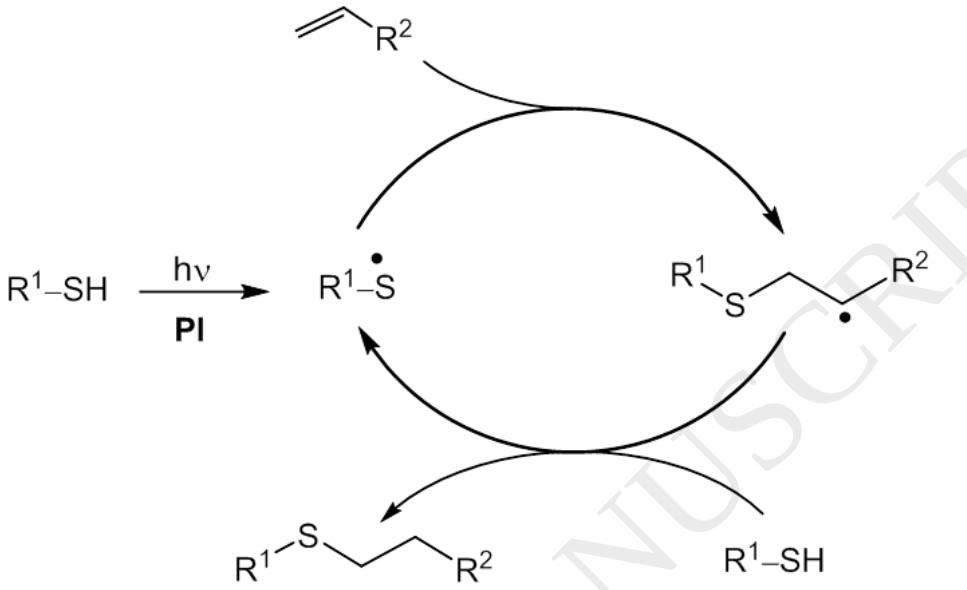

Scheme 1. The photochemical radical thiol-ene addition mechanism (PRTEA).

ACCEPTED MANUSCRIPT

ACCEPTED MANUSCRIPT

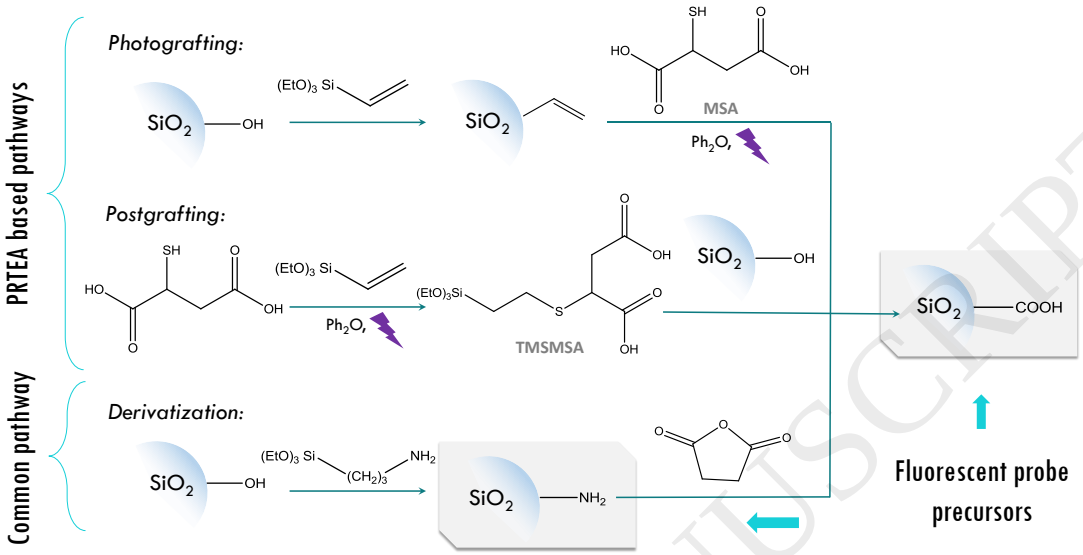

Scheme 2. Different chemical routes used to obtain the SiO_2-COOH .

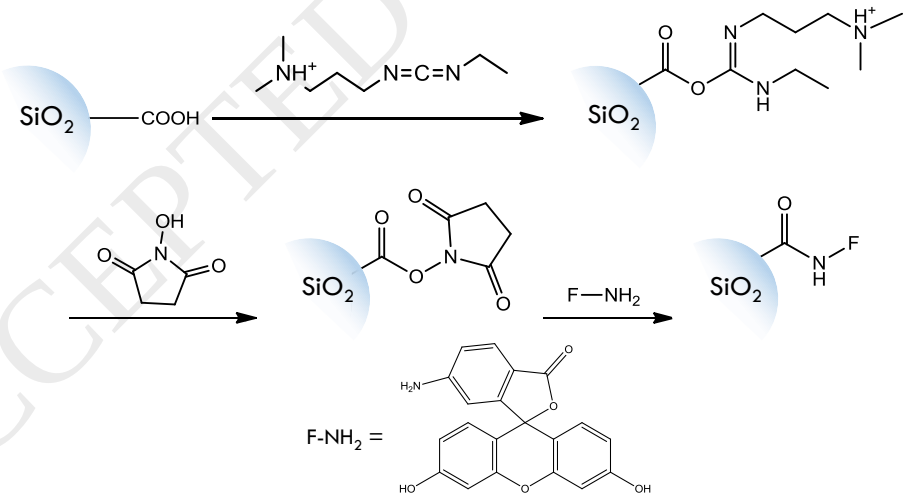

Scheme 3. Chemical reaction steps involved in the binding of fluorescein to SiO_2-COOH NPs using EDC / NHS.

ACCEPTED MANUSCRIPT

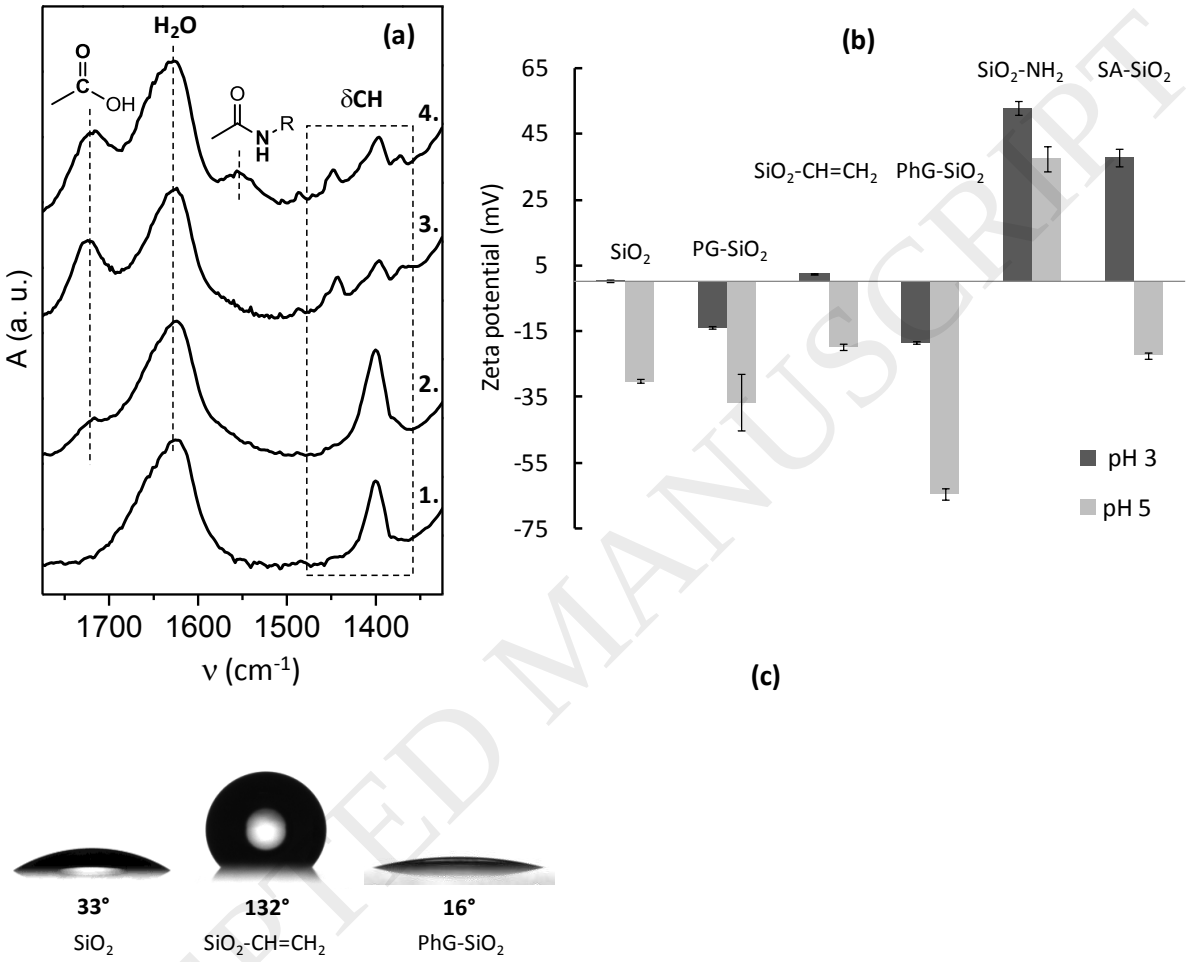

Figure 1. (a) FTIR spectra of: bare SiO_2 NPs (1), PhG-SiO_2 (2), PG-SiO_2 (3) and SA-SiO_2 NPs (4). **(b)** Zeta potential of the bare SiO_2 NPs, modified with intermediate functional group (vinyl and amino), and SiO_2-COOH NPs synthesized by the three different pathways. **(c)** Images of the sessile drop of water on colloidal films of the NP belonging to the photografting series and their contact angle.

ACCEPTED MANUSCRIPT

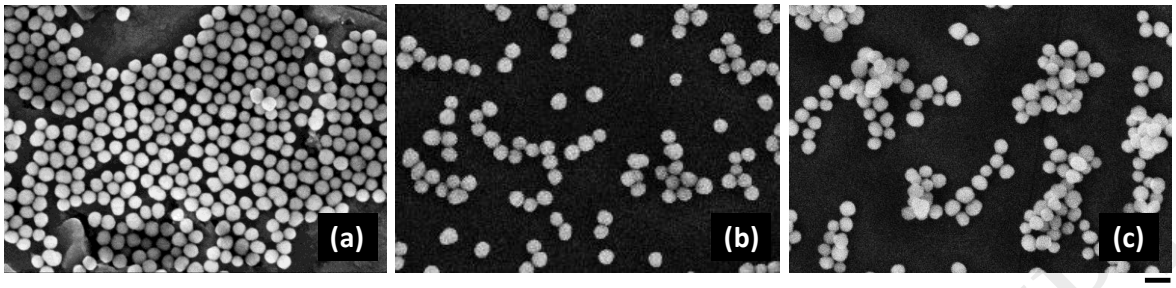

Figure 2. FESEM micrographs of (a) starting bare SiO_2, (b) PG-SiO_2 and (c) SiO_2-NH_2 NPs. The scale bar indicates 100 nm.

ACCEPTED MANUSCRIPT

ACCEPTED MANUSCRIPT

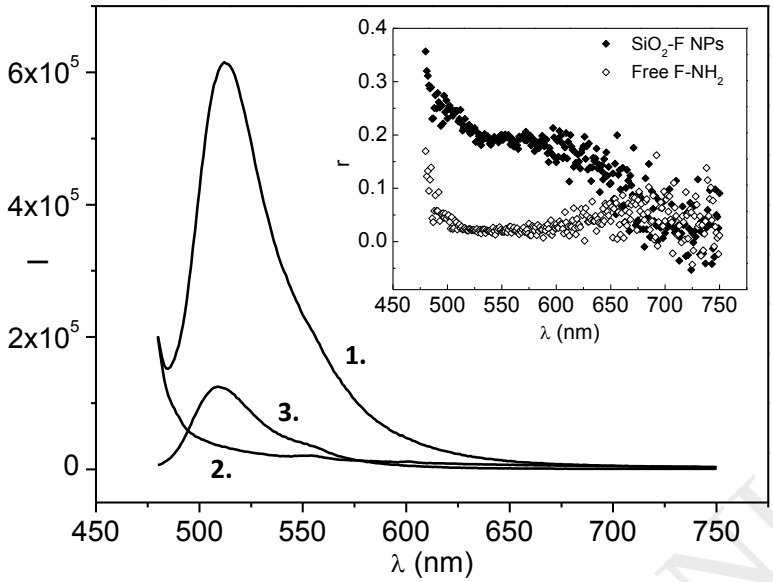

Figure 3. Fluorescence spectra of the NPs obtained after the derivatization of PhG-SiO_2 NPs with F-NH_2/EDC/NHS (1), PhG-SiO_2 NPs with F-NH_2 and no EDC/NHS (2) and free F-NH_2/EDC/NHS and no PhG-SiO_2 NPs. Inset: Fluorescence anisotropy of free F-NH_2 and NP-bound F-NH_2.

ACCEPTED MANUSCRIPT

ACCEPTED MANUSCRIPT

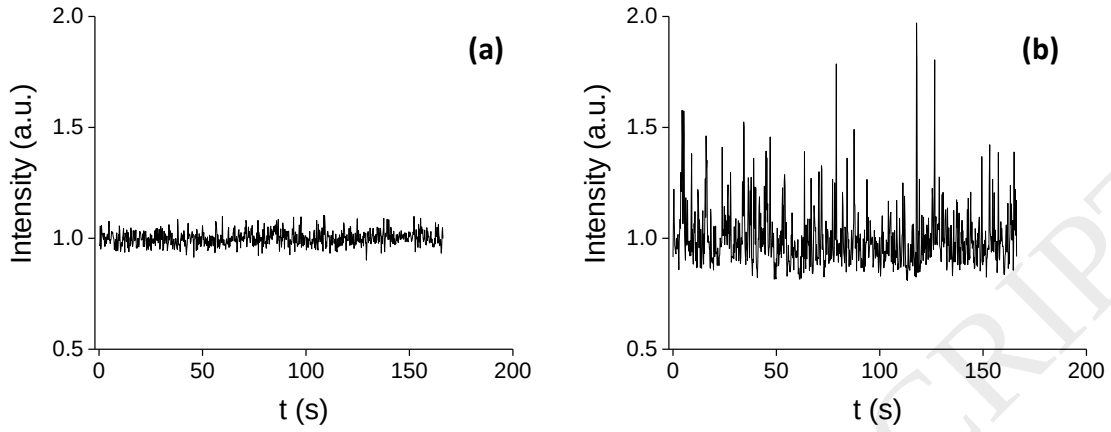

Figure 4. Typical normalized fluorescence intensity fluctuations: PhG-SiO_2 NPs (a) and PG-SiO_2 NPs (b).

ACCEPTED MANUSCRIPT

ACCEPTED MANUSCRIPT

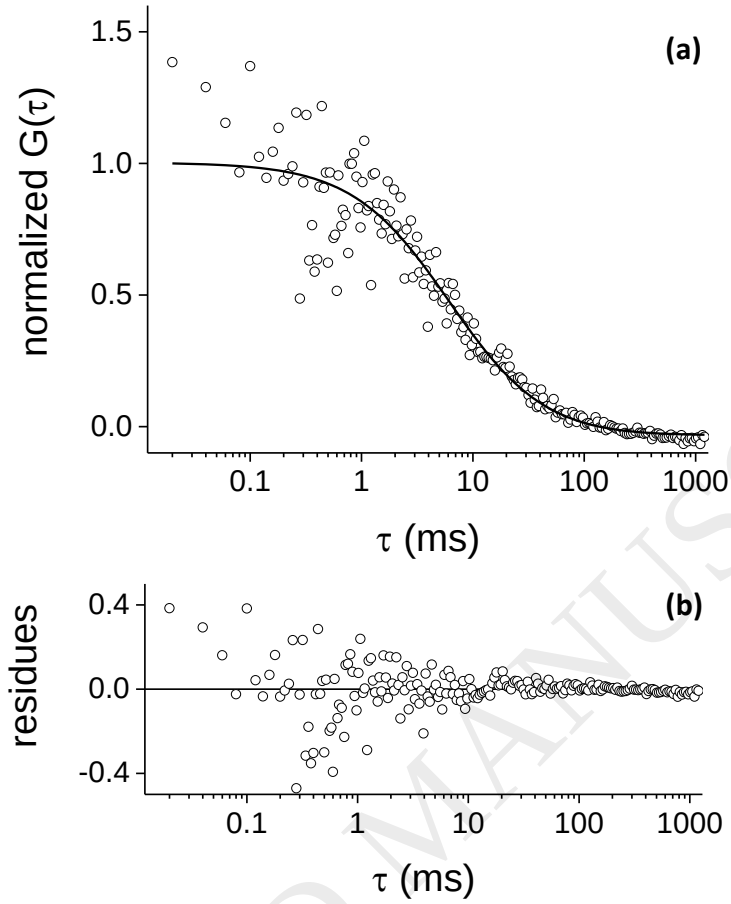

Figure 5. Autocorrelation function G(t) for PhG-SiO_2 NPs (a) and fitting residues (b). (○: experimental data, solid line: fit to Equation 5)

Table 1. Estimated grafting density of surface terminal groups, δ_{exp}, from thermogravimetric experiments and Equation 1.

NP	**δ_{exp} / nm^{-2}**	**δ_{COOH} / nm^{-2}**
SiO_2-CH=CH_2	3.2	-
PhG-SiO_2	2.5	4.9
PG-SiO_2	1.8	3.6
SiO_2-NH_2	4.9	-
SA-SiO_2	2.0	2.0

Table 2. Ratio between the hydrodynamic diameter obtained by DLS for the modified NPs with the intermediate functional groups, vinyl and amino, and for the SiO_2-COOH NPs obtained by the

ACCEPTED MANUSCRIPT

different pathways, and the hydrodynamic diameter of the respective unmodified starting SiO_2 NPs.

SiO_2-COOH synthesis pathway					
Photografted		**Post-grafted**		**Derivatized**	
$\frac{D_{H,SiO_2-CH=CH_2}}{D_{H,SiO_2}}$	1,02 ± 0,05	$\frac{D_{H,PG-SiO_2}}{D_{H,SiO_2}}$	1,13 ± 0,07	$\frac{D_{H,SiO_2-NH_2}}{D_{H,SiO_2}}$	2,6 ± 0,6
$\frac{D_{PhG-SiO_2}}{D_{H,SiO_2}}$	1,02 ± 0,06			$\frac{D_{H,SA-SiO_2}}{D_{H,SiO_2}}$	1,8 ± 0,1

Table 3. Ratio between the hydrodynamic diameter obtained by DLS for the SiO_2 and PhG-SiO_2 NPs in the reconstituted suspensions, $D_{H,R}$, and the initial one, $D_{H,i}$.

	$\frac{D_{H,R}}{D_{H,i}}$	
	SiO_2	PhG-SiO_2
Frozen NP	1,2 ± 0,2	1,07 ± 0,05
Dry NP	1,2 ± 0,4	1,07 ± 0,04

Table 4. Ratio between the D_H from FCS and DLS for the modified F-SiO_2 NPs obtained by the different synthesis pathways. (*) Ratio after correcting the measured correlation time τ_c according to Equation 7. *Agg.:aggregates*

	$\frac{D_{H,FCS}}{D_{H,DLS}}$	$\frac{D_{H,FCS}}{D_{H,DLS}}$ (*)
F-PhG-SiO_2	1,19	1,14
F-PG-SiO_2	1,24	1,05
F-SA-SiO_2	*Agg.*	*Agg.*
F-CO-NH-SiO_2	*Agg.*	*Agg.*

ACCEPTED MANUSCRIPT